

Conformational transitions monitored for single molecules in solution

LARS EDMAN, ÜLO METS*, AND RUDOLF RIGLER†

Department of Medical Biophysics, Karolinska Institute, S-171 77 Stockholm, Sweden

Communicated by Hans Frauenfelder, Los Alamos National Laboratory, Los Alamos, NM, February 27, 1996 (received for review December 20, 1995)

ABSTRACT Phenomena that can be observed for a large number of molecules may not be understood if it is not possible to observe the events on the single-molecule level. We measured the fluorescence lifetimes of individual tetramethylrhodamine molecules, linked to an 18-mer deoxyribonucleotide sequence specific for M13 DNA, by time-resolved, single-photon counting in a confocal fluorescence microscope during Brownian motion in solution. When many molecules were observed, a biexponential fluorescence decay was observed with equal amplitudes. However, on the single-molecule level, the fraction of one of the amplitudes spanned from 0 to unity for a collection of single-molecule detections. Further analysis by fluorescence correlation spectroscopy made on many molecules revealed a process that obeys a stretched exponential relaxation law. These facts, combined with previous evidence of the quenching effect of guanosine on rhodamines, indicate that the tetramethylrhodamine molecule senses conformational transitions as it associates and dissociates to a guanosine-rich area. Thus, our results reveal conformational transitions in a single molecule in solution under conditions that are relevant for biological processes.

A new era of molecular analysis was begun by the introduction of extremely sensitive methods to detect and characterize species at the single-molecule level by spectroscopic means. Several techniques to trace individual fluorescent particles in solution have been reported over the last 12 years (1–9). Single-molecule detection (SMD) in solids and on surfaces has also been accomplished (10–14); however, many features important for chemical and biological systems can only be realized in the liquid phase, as is pointed out by reports regarding applications in DNA sequencing (15, 16) or detection and selection of rare events in diagnostics and biotechnology (17). Another important application for the SMD technique is the study of reaction dynamics at the single-molecule level.

Wang and Wolynes (18) have recently reported how measurements of single molecules can make it possible to gain information about phenomena that cannot be easily understood when a large number of molecules are observed simultaneously. A complex behavior (e.g., a distribution of a physical entity) will not provide information on whether all molecules share a common distribution or whether each molecule gives its own specific contribution to the distribution seen for many molecules. Measurements of single molecules can be decidedly important in obtaining such information.

Previously, measurements of fluorescence lifetimes for single molecules in solution have been achieved by the use of a flowing sample stream, for which one fluorescence lifetime was apparent (19, 20). We present the results from experiments in which the fluorescence lifetimes of individual molecules undergoing Brownian motion have been measured by confocal

illumination and detection (3, 5). The finding that tetramethylrhodamine (TMR) molecules linked to an 18-mer oligonucleotide can emit fluorescence with two different lifetimes suggests the existence of a two-spectroscopic-state process (TSSP) at the single-molecule level.

MATERIALS AND METHODS

Sample Molecule. All experiments were performed with a TMR-labeled sequencing primer (5'TGTAACACGACGGC-CAGT3', NAPS, Göttingen, Germany) for which one complementary sequence is found in M13 mp18(+)strand DNA (7250 bases). The fluorophore was bound to the oligonucleotide by a six-carbon-atom linker at the 5' end. The rhodamine-labeled primer interacted with a complementary sequence of M13 DNA. The DNA served only as an additional mass coupled to the primer to make the complex molecule move slower during its Brownian motion.

Fluorescence Decay (FD) and Fluorescence Correlation Spectroscopy (FCS) Measurements. The experimental setup has been described (21), but some modifications were made. We used a modified single-photon-counting diode with fast signal output (EG & G Optoelectronics, Canada; model SPCM-211) for FCS and FD measurements. A mode-locked Ar⁺ laser operated at a frequency of 76.7 MHz with a wavelength of 515 nm was used. FD measurements were taken with the use of time-correlated, single-photon counting with a time to amplitude converter and a pulse height analyzer, and FCS measurements were taken with the use of a digital correlator (ALV, Germany; model ALV-5000). The pulse rate of the laser exceeded by far the inverse of the characteristic time for molecular passages through the observable volume element (VE) from where the light is detected. Comparison of data obtained from CW-excitation experiments shows that changing the laser from continuous to pulsed operation does not affect the FCS measurements. We did not need FCS to detect the molecules, as has been assumed (22), but we used it as a sensitive instrument to provide precise statistical characteristics of the system.

Single-Molecule Measurements. To achieve SMD, we measured repeatedly for short periods (*t*). The ratio of the measurement time to the characteristic passage time of a molecule through the VE is defined as *T*, the relative measuring time. By selecting only those measurements that experienced a large time integral of the detected fluorescence, we could effectively make a discrimination between clear single-molecule events and blanks (Fig. 1).

The probability of a single molecule passing into the VE in a short time interval (*dt*) is calculated by $(N/\tau_{\text{diff}})dt + o(dt)$,

Abbreviations: SMD, single-molecule detection; TMR, tetramethylrhodamine; TSSP, two-spectroscopic-state process; FD, fluorescence decay; FCS, fluorescence correlation spectroscopy; VE, volume element; ACF, autocorrelation function.

*Present address: Institute of Chemical Physics and Biophysics, Tallinn, Estonia.

†To whom reprint requests should be addressed.

The publication costs of this article were defrayed in part by page charge payment. This article must therefore be hereby marked "advertisement" in accordance with 18 U.S.C. §1734 solely to indicate this fact.

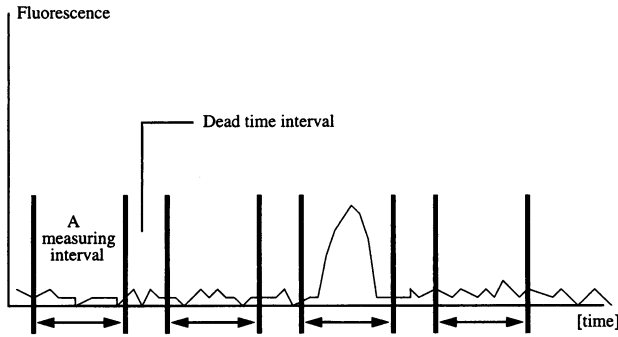


FIG. 1. Principal time schedule for the FD SMD measurements. An SMD event is characterized by a larger value of the integrated fluorescence in a measuring interval.

where N is the relative concentration of the molecules per one VE, τ_{diff} is the characteristic passage time for a molecule, and o is the “small ordo” function. Molecules enter the VE in a purely random order and are independent of all other particles’ behavior. The probability of more than one molecule passing in the time interval dt is shown by $o(dt)$. A general expression for the probability of n molecules entering the VE within a time interval t will then be

$$P_n^e(t, \tau_{\text{diff}}, N) = P_n^e\left(t \frac{N}{\tau_{\text{diff}}}\right) = P_n^e(NT) = \frac{(NT)^n}{n!} e^{-NT}. \quad [1]$$

The probability of n molecules residing in the VE at one instance can be calculated in analogy with the above case by assuming a probability dN for one molecule in the VE for a small relative molecular concentration dN ,

$$P_n^r(N) = \frac{N^n}{n!} e^{-N}. \quad [2]$$

To finally obtain the expression for the n -molecule probability in a time interval t , $P_n(N, T)$, the two probability distributions are convoluted,

$$P_n(N, T) = \sum_{i=0}^n P_i^r(N) P_{n-i}^e(NT). \quad [3]$$

Thus, the probability (p) of a single-molecule event in a measurement depends on the specific sample concentration, N (molecules/VE), as well as the relative measuring time, T (measuring time/characteristic diffusion time), via the expression

$$p_{n=1} = P(\text{SMD in a measurement}) = N(1+T)e^{-N(1+T)}. \quad [4]$$

The probability (p) of two or more molecules residing inside the VE during an SMD measurement time interval is calculated by

$$p_{n>1} = P(\text{multimolecular measurement}) = 1 - e^{-N(1+T)}[1 + N(1+T)]. \quad [5]$$

The fraction (F) of the measurements that are accepted as SMD events should not be in the same order of magnitude as the value for $p_{n>1}$ (Eq. 5). If this is the case, the measurements will on the average originate not from a single molecule, but from two or more. On the other hand, it is appropriate to let F be slightly less than $p_{n=1}$ to accept only those molecules that are not photobleached (23), and also diffuse for a large time and/or in the central part of the VE, where the excitation light has the largest intensity. The tradeoff between distinct SMD data and a low fraction of multimolecular events in the

measurements was the most important factor in the completion of our SMD experiment.

Data Analysis and Theoretical Models. In FCS, molecules in a very small open volume (0.2–100 fl) are excited by a CW laser, and the autocorrelation function (ACF) of the fluorescence intensity is computed. The ACF describes the average behavior of individual molecules, since fluorescence from different noninteracting molecules is completely uncorrelated. Therefore, the condition of only one molecule in the observation volume is not necessary for FCS. For obtaining an ACF with high signal-to-noise ratio, a large number of single-molecule events must be averaged. In this work, FCS was used for two purposes. First, FCS allowed us to precisely determine the absolute average number of fluorescent molecules in the VE as well as the average diffusion time through the VE. Further on, we used it to assess the exchange rate between the states with different excited state lifetimes. This is possible since a change in the lifetime is accompanied by a corresponding change in the quantum yield and brings about an additional component in the ACF, provided that the exchange rate is faster than diffusion through the VE.

The FCS measurements for determining the number of molecules and diffusion time were taken under identical conditions to the SMD experiments (radius of the VE, $w_0 = 0.6 \mu\text{m}$). In measurements of the exchange rates, w_0 was increased to $2.2 \mu\text{m}$ to achieve a longer diffusion time (250 ms), and the laser intensity was adjusted such that the average time to photobleach a TMR molecule was longer than 1 s. In FCS, the fluorescence intensity at time t , $I(t)$, is correlated with the fluorescence at time $t + \tau$. The normalized autocorrelation function can generally be written as

$$G(\tau) = \frac{\langle I(t)I(t+\tau) \rangle}{\langle I^2 \rangle} = \frac{\langle [I(t) + \delta I(t)][I(t+\tau) + \delta I(t+\tau)] \rangle}{\langle I^2 \rangle}. \quad [6]$$

In Eq. 6, $\langle \rangle$ indicates ensemble average, and $\delta I(t)$ is the intensity fluctuation from the mean value at time t .

The FCS data were analyzed according to models for which an extensive documentation already exist (4, 21, 24, 25). However, nothing has yet been published regarding FCS applied on stretched exponential processes (26, 27). Starting from the analysis of unimolecular transitions published previously (24), transitions involving stretched exponentials have been formulated accordingly (Eq. 7). When the characteristic passage time for a molecular transition through the VE is larger than the characteristic time of the monitored process, a proper model is

$$G(\tau) = \frac{1}{N} \frac{1}{1 + \frac{4D}{w^2} \tau} \frac{1}{\sqrt{1 + \frac{4D}{z^2} \tau}} (1 + Ae^{-(k\tau)^\beta}) + 1, \quad [7]$$

where N is the average number of molecules per VE and D is the diffusion coefficient. The e^{-2} intensity drop distance from the laser excitation focus is w in the radial direction and z in the direction of the optical axis of the beam. The characteristic diffusion time, or passage time for the molecule through the VE, is defined as $\tau_{\text{diff}} = w^2/4D$. β is the “stretch” parameter (27), k is a reaction relaxation parameter, and A is a constant whose magnitude depends on the quantum yield difference between the two states, as well as the equilibrium constant between the two states through the expression

$$A = K \left(\frac{1-Q}{1+QK} \right)^2, \quad [8]$$

where K is the equilibrium constant and Q is the quantum yield ratio of the two states.

The fluorescence decays were modelled as a superposition of two exponential functions, with different decay values ($\tau_{1,2}$) and amplitudes ($a_{1,2}$),

$$a_1 e^{-\frac{t}{\tau_1}} + a_2 e^{-\frac{t}{\tau_2}} \quad [9]$$

The decay model was convoluted with the instrumental response function before data analysis was performed.

The Marquardt–Levenberg nonlinear least-squares algorithm (28) was applied in all cases for optimization.

RESULTS

The characteristic passage time for the molecule through the VE was derived from FCS measurement data to 22 ms.

FD measurements were first accomplished with 25 nM solution equivalent to 60 molecules per VE. Because of the large number of fluorophores, the laser power was held low at 25 μ W. To get precise statistics (29), we recorded a large amount of fluorescence ($\approx 10^7$ counts). Two lifetimes were evident: $\tau_1 = 0.86 \pm 0.02$ ns and $\tau_2 = 3.70 \pm 0.07$ ns, with a fraction of 0.55 ± 0.04 for the longer lifetime (Fig. 2). The fraction of τ_2 is defined as $a_2/(a_1 + a_2)$. Models with one exponential lifetime failed to apply to the FD data, and the use of three or more exponentials in the model did not introduce any additional lifetime, nor did it improve the fit, based on χ^2 distributed residuals ($\chi^2 = 0.982$).

In the SMD part, we used a 2.5 pM sample solution, which corresponds to 0.006 molecules per VE. To get a sufficient amount of fluorescence from single fluorophores, the laser power had to be increased to 0.5 mW. The measurement time interval (t) was set to 30 and 80 ms. We selected the threshold of the time integral of the fluorescence in each SMD measurement to a value such that F equalled 0.0025 and 0.0017, respectively. The corresponding multimolecular probability as given by Eq. 5 was 0.00010 and 0.00038, respectively; thus, we concluded that only distinct SMD were recorded ($p_{n=1}/F = 5.59$ and 15.91, respectively) without the incorporation of a significant fraction of multimolecular events, $p_{n>1}/F = 0.04$ and 0.22, respectively, indicating

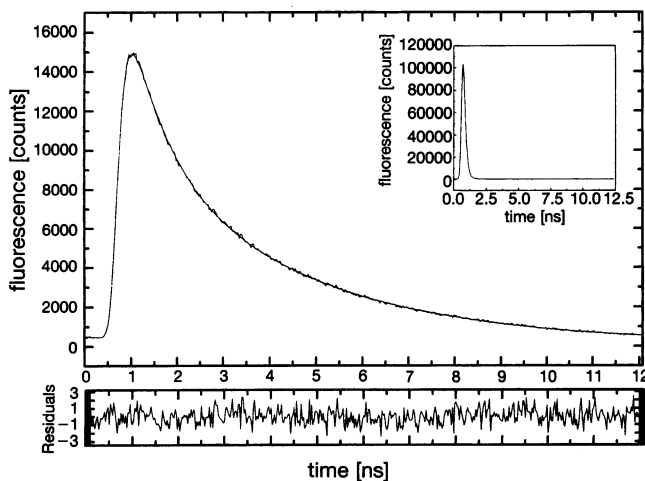


FIG. 2. Measurement data recorded when 25 nM sample solution was measured for a long time. A model fit, including two exponential terms, is shown as a line through the observed data. In the model, the complete convolution process, as well as a Raman scattering term and a background term, was included to get an optimal model-to-reality correspondence. Two exponential lifetimes were surveyed, $\tau_1 = 0.86$ ns and $\tau_2 = 3.70$ ns. The lower panel shows the residuals between the observed data and the calculated model data. (Inset) Instrumental response function.

that in about 4% and 22% of the measurements, there was some influence from an additional fluorophore.

For the analysis of single-molecule events, a minimum of 200 and 600 counts were collected in the 30- and 80-ms experiments, respectively. The presence of one or two lifetimes was assessed by determining the fraction of τ_2 , with τ_1 and τ_2 fixed to the values determined from experiments on many molecules.

Contrary to the FD measurements taken for a large number of molecules, the SMD FD data showed a distribution of the recorded fraction of τ_2 for a collection of measurement intervals, covering all fractions from 0 to unity (30). For simulated SMD measurement data, the mean error of the fraction of τ_2 was determined to 0.13 (30 ms) and 0.06 (80 ms) (30). For some measurements, only one lifetime was recorded (Fig. 3A–D); however, in most measurements, counts from the two lifetimes were present at different relative quantities.

When we used FCS to monitor the conformational transitions as observed by fluctuations of the quantum yield of two states for many molecules simultaneously, the VE had to be enlarged. The characteristic passage time in these measurements was 250 ms, which provided for a larger time scale to be used as the process was observed (Fig. 4). The stretched exponential-specific parameters were evaluated by the use of Eq. 7 to $A = 0.38 \pm 0.04$, $\beta = 0.44 \pm 0.04$, and $k^{-1} = 23 \pm 13$ ms. The large error in the evaluation of the relaxation parameter k is most probably due to the fact that the stretched exponential distribution has a flat appearance (for $\beta < 1$). It is “stretched out,” thereby distributing the probability density over a much wider area, which makes the analysis more demanding. Thus, the flatness will make it hard to make a detailed data analysis of the parameter k . The dimensions of the VE (i.e., the parameters z and w in Eq. 7) could be determined in separate FCS measurements made on rhodamine 6G. The presence of a simple two-state transition ($\beta = 1$) was excluded by comparing the χ^2 distributed residuals.

DISCUSSION

The character of these findings gives only one conceivable conclusion, that the fluorophore undergoes a process in which the lifetime alternates between τ_1 and τ_2 in the course of time. The two lifetimes that were observed in the FD measurements can be explained by the photophysical property of guanosine on rhodamines in general. It has been shown (31, 32) that, among the four nucleotide bases, guanosine quenches rhodamines profoundly, and no other nucleotide base will accomplish this. These facts make us believe that the shorter lifetime emerges from the instances in which the TMR molecule is situated in the vicinity of a guanosine-rich area. This will make it possible for an electron transfer mechanism to become a strong competitor to the fluorescence process; thus, the lifetime will be reduced when the excitation energy is lost more often without the birth of a photon. The distribution of lifetimes of TMR linked to the primer containing several guanosine residues is the same in the absence and presence of cDNA. This indicates that the additional mass used to slow down the diffusion process does not influence the distribution of states exhibited by TMR.

We have introduced the stretched exponential relaxation function in the FCS measurements. The characteristics of processes that obey this relaxation law are, in general, processes in complex systems where a transition from one state to the other depends on a number of subprocesses. These subprocesses must always be completed before the main process changes its state. Mathematically, this has been formulated in a very elegant manner by Palmer and coworkers (26). By introducing a hierarchical substate model, they showed that the main process will obey a stretched exponential relaxation behavior for certain choices of the model parameters. Conformational transitions are characterized as an outcome from numerous subprocesses, all of which make the transition possible. As is pointed out

by Frauenfelder and coworkers (27), for the special case of protein molecules, a stretched exponential behavior is to be expected from complex conformational transitions.

The knowledge of the origin of the small lifetime, as well as the reaction time distribution for the TSSP, and especially the times when such distributions arise, encouraged us to make a further conclusion. A proper model to describe the physical nature behind the TSSP can be formed. The TMR molecule is linked to the oligonucleotide by the carbon chain. Occasionally, this chain configures itself according to a conformation such that contact will be acquired between the fluorophore

and guanosine. A model prototype is outlined in Fig. 5. The TSSP will have its origin in a conformational transition process. In state 2 the TMR molecule is photophysically unaffected and emits fluorescence with lifetime τ_2 . When a transition is made to state 1, the lifetime of the TMR molecule is quenched by means of electron transfer between guanosine and the fluorophore. The lifetime will thus be reduced in state 1.

The inverse of the lifetime equals the rate of the depopulation of the excited state of the fluorophore, $\tau^{-1} = k = k_r + k_{nr}$. Here, k_r is due to fluorescence and k_{nr} is the sum of all other depopulation processes.

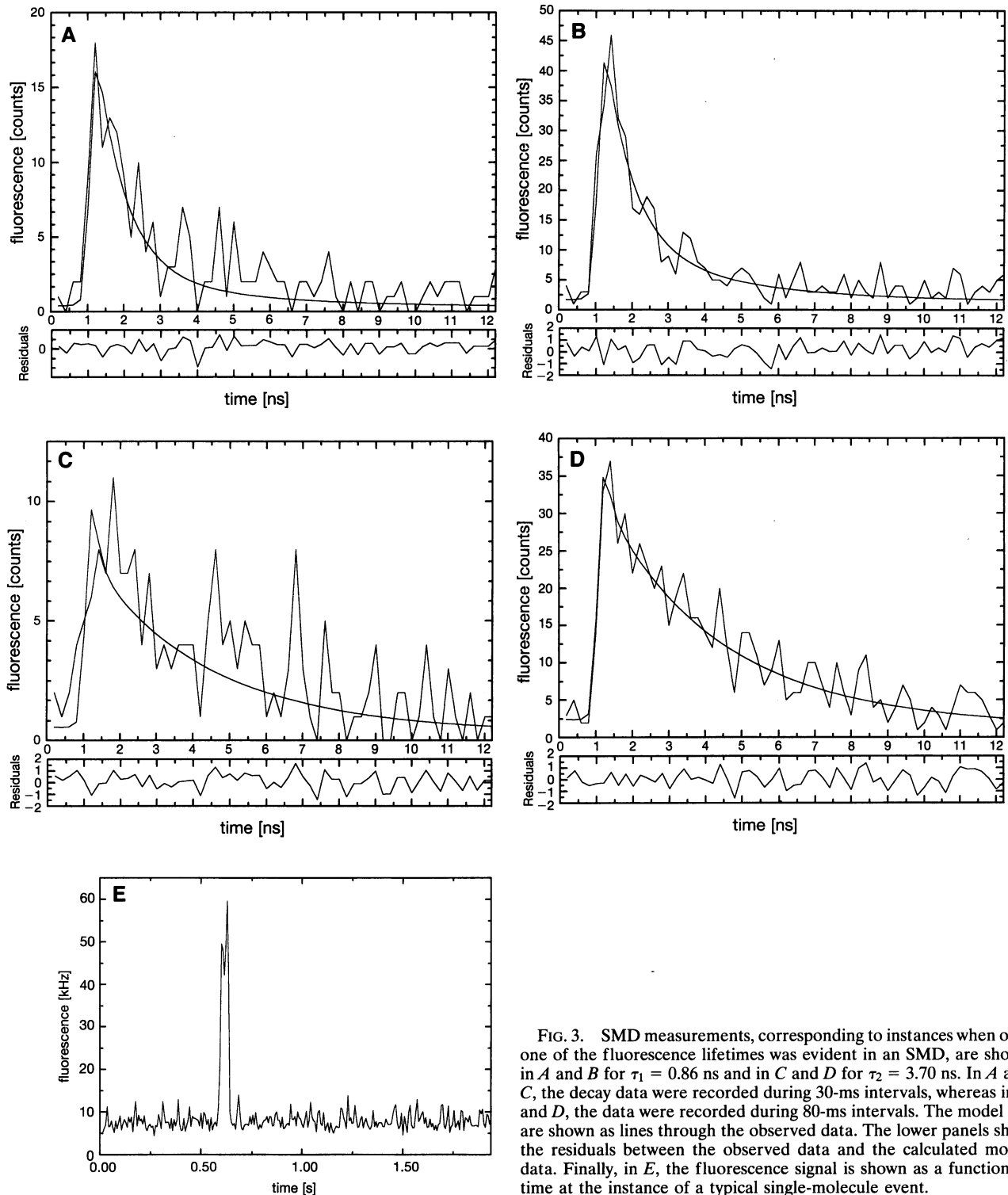


FIG. 3. SMD measurements, corresponding to instances when only one of the fluorescence lifetimes was evident in an SMD, are shown in *A* and *B* for $\tau_1 = 0.86$ ns and in *C* and *D* for $\tau_2 = 3.70$ ns. In *A* and *B*, the decay data were recorded during 30-ms intervals, whereas in *C* and *D*, the data were recorded during 80-ms intervals. The model fits are shown as lines through the observed data. The lower panels show the residuals between the observed data and the calculated model data. Finally, in *E*, the fluorescence signal is shown as a function of time at the instance of a typical single-molecule event.

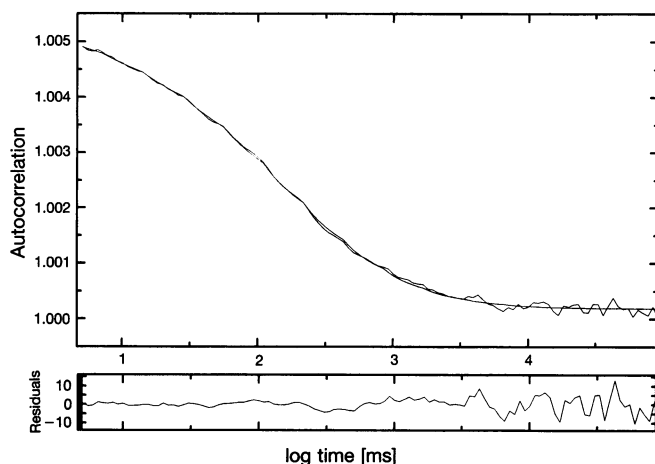


FIG. 4. Autocorrelation function $G(\tau)$ of the fluorescence intensity fluctuation due to conformational transitions and diffusion. Recorded and fitted data (Eq. 7) with residuals. The volume element has been enlarged to give a diffusion time of $\tau_D = 250$ ms.

Under the assumption that k_r is constant for the fluorophore at all times, the quantum yield ratio of the two states is given by $\tau_1/\tau_2 = 0.86/3.70 \approx 0.23$, which is the value of Q in Eq. 7. We can now solve for K in Eq. 7, since the FCS measurements has provided the value of A . The derived value of K is approximately unity, which indicates that the fluorophore resides for a roughly equal time in states 1 and 2, in agreement with $a_1 \approx a_2 \approx 0.5$ from the ensemble measurement.

From the work of Frauenfelder and coworkers on the photodissociation and rebinding of CO to myoglobin, the picture of conformational substates (33, 34) emerged, giving rise to distributed kinetics (27, 34). Although we found strong evidence for the existence of widely distributed exchange rates, as seen from the stretched exponential behavior in the FCS data, we did not observe the existence of multiple substates in the FD data. Only two distinct states are observed, even if the data are analyzed for the existence of distributed exponentials. A likely explanation is that, despite the existence of a variety of substates, only two can be observed. The transition from one state to the other thus takes place through a hypersurface in conformational space.

The influence of the environment on single dye molecules dispersed on surfaces has been demonstrated by lifetime and spectral analysis using near-field detection (10–12). Recent reports have demonstrated that single molecules are involved in slow enzymatic turnovers (8) as well as in chemical reactions (9). Biological processes are often confined to time scales that are much less than 1 s, and the importance of monitoring such processes in their characteristic time scale cannot be overes-

timated. Here, a complex molecular reversible process, involving conformational transitions at the single-molecule level in solution, has been measured in the same time scale as its natural relaxation rate and in the natural surroundings of the molecule, i.e., in aqueous solution.

We thank Dr. Per Thyberg for the analysis of distributed exponentials and Dr. Jerker Widengren for discussions. This study was supported by grants from the Swedish Natural Science Research Council and the Swedish Research Council for Engineering Sciences.

1. Dovichi, N. J., Martin, J. C., Jett, J. H., Trkula, M. & Keller, R. A. (1984) *Anal. Chem.* **56**, 348–354.
2. Shera, E. B., Seitzinger, N. K., Davis, L. M., Keller, R. A. & Soper, S. A. (1990) *Chem. Phys. Lett.* **174**, 553–557.
3. Rigler, R. & Mets, Ü. (1992) *SPIE Laser Spectrosc. Biomol.* **1921**, 239–248.
4. Rigler, R., Widengren, J. & Mets, Ü. (1993) in *Fluorescence Spectroscopy: New Methods and Applications*, ed. Wolfbeis, O. S. (Springer, Berlin), pp. 13–24.
5. Mets, Ü. & Rigler, R. (1994) *J. Fluorescence* **4**, 259–264.
6. Whitten, W. B., Ramesey, J. M., Arnold, S. & Bronk, B. V. (1991) *Anal. Chem.* **63**, 1027–1031.
7. Fan, F. F. & Bard, A. J. (1995) *Science* **267**, 871–874.
8. Funatsu, T., Harada, Y., Tokunaga, M., Salto, K. & Yanagida, T. (1995) *Nature (London)* **374**, 555–559.
9. Collinson, M. M. & Wightman, R. M. (1995) *Science* **268**, 1883–1885.
10. Xie, X. S. & Dunn, R. C. (1994) *Science* **265**, 361–364.
11. Ambrose, W. P., Goodwin, P. M., Martin, J. C. & Keller, R. A. (1994) *Science* **265**, 364–367.
12. Trautman, J. K., Macklin, J. J., Brus, L. E. & Betzig, E. (1994) *Nature (London)* **369**, 40–42.
13. Basché, T., Kummer, S. & Bräuchle, C. (1995) *Nature (London)* **373**, 132–134.
14. Basché, T. & Moerner, W. E. (1992) *Nature (London)* **355**, 335–337.
15. Goodwin, P. M., Schecker, J. A., Wilkerson, C. W., Hammond, M. L., Ambrose, W. P., Jett, J. H., Martin, J. C., Marrone, B. L. & Keller, R. A. (1993) *SPIE Adv. DNA Sequencing Tech.* **1891**, 127–131.
16. Köllner, M. (1993) *Appl. Optics* **32**, 806–820.
17. Eigen, M. & Rigler, R. (1994) *Proc. Natl. Acad. Sci. USA* **91**, 5740–5747.
18. Wang, J. & Wolynes, P. (1995) *Phys. Rev. Lett.* **74**, 4317–4320.
19. Tellinghulsen, J., Goodwin, P. M., Ambrose, W. P., Martin, J. C. & Keller, R. A. (1994) *Anal. Chem.* **66**, 64–72.
20. Soper, S. A., Davis, L. M. & Shera, E. B. (1992) *J. Opt. Soc. Am. B* **9**, 1761–1769.
21. Rigler, R., Mets, Ü., Widengren, J. & Kask, P. (1993) *Eur. Biophys. J.* **22**, 169–175.
22. Nie, S., Chiu, D. T. & Zare, R. N. (1994) *Science* **266**, 1018–1021.

M13 DNA

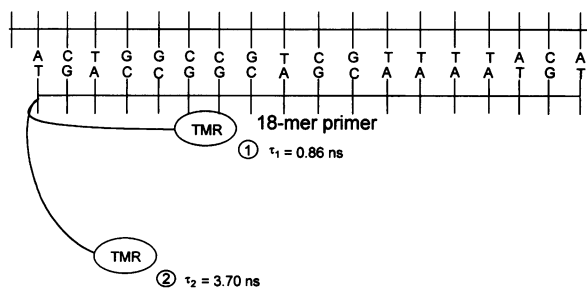


FIG. 5. Model of the conformational transition process. The two states 1 and 2 are characterized by their individual fluorescence lifetime. State 2 represent the cases in which no contact between TMR and guanine is acquired. The length of the carbon linker enables contact between the TMR molecule and guanine when the linker is stretched along the oligonucleotide.

23. Whitten, W. B. & Ramsey, J. M. (1992) *Appl. Spectrosc.* **46**, 1587–1589.
24. Elson, E. & Magde, D. (1974) *Biopolymers* **13**, 1–27.
25. Thompson, N. L. (1991) in *Topics in Fluorescence Spectroscopy*, ed. Lakowicz, J. R. (Plenum, New York), Vol. 1, pp. 337–378.
26. Palmer, R. G., Stein, D. L., Abrahams, E. & Anderson, P. W. (1984) *Phys. Rev. Lett.* **54**, 958–961.
27. Frauenfelder, H., Sligar, S. G. & Wolynes, P. G. (1991) *Science* **254**, 1598–1603.
28. Marquardt, D. (1963) *J. Soc. Ind. Appl. Math.* **11**, 431–441.
29. Köllner, M. & Wolfrum, J. (1992) *Chem. Phys. Lett.* **200**, 199–203.
30. Edman, L., Mets, Ü. & Rigler, R. (1996) *Exp. Tech. Phys.*, in press.
31. Sauer, M., Han, K.-T., Muller, R., Nord, S., Schulz, S. Wolfrum, J., Arden-Jacob, J., Deltau, G., Marx, N. J., Zander, C. & Drexlyhage, K. H. (1995) *J. Fluorescence* **5**, 247–261.
32. Widengren, J. (1996) Ph.D. thesis (Karolinska Institute, Stockholm).
33. Austin, R. H., Beeson, K. W., Eisenstein, L., Frauenfelder, H. & Gunsalus, I. C. (1975) *Biochemistry* **14**, 5355–5373.
34. Frauenfelder, H., Parak, F. & Young, R. D. (1988) *Annu. Rev. Biophys. Chem.* **17**, 451–479.